

**INORGANIC SYNTHESIS  
AND INDUSTRIAL INORGANIC CHEMISTRY**

**Synthesis of ZSM-12 Zeolites with New Templates  
Based on Salts of Ethanolamines**

**D. E. Tsaplin<sup>a</sup>, D. A. Makeeva<sup>a</sup>, L. A. Kulikov<sup>a,b,\*</sup>, A. L. Maksimov<sup>a,b</sup>, and E. A. Karakhanov<sup>a</sup>**

<sup>a</sup> Lomonosov Moscow State University, Moscow, 119991 Russia

<sup>b</sup> Topchiev Institute of Petrochemical Synthesis, Russian Academy of Sciences, Moscow, 119991 Russia

\*e-mail: mailforleonid@mail.ru

Received October 9, 2018

**Abstract**—New class of templates, ethanolamine salts, was used to synthesize zeolites with the ZSM-12 structure. The materials obtained were characterized by methods of powder X-ray diffraction, scanning electron microscopy, IR spectroscopy, low-temperature adsorption–desorption of nitrogen, and elemental analysis. It was shown that, with these templates, it is possible to obtain crystallites with well formed acicular shape, hexagonal morphology, large surface area, and narrow pore size distribution.

**Keywords:** zeolites, ZSM-12, ethanolamines, hydrothermal synthesis

**DOI:** 10.1134/S1070427218120066

Xylenes are among the most industrially valuable substances, which serve as raw materials for synthesis of dyes and plasticizers and are used as solvents. Of particular importance among these substances is para-xylene used to synthesize terephthalic acid for subsequently obtaining synthetic polymeric fibers. Therefore, the demand for para-xylene substantially exceeds that for other xylenes.

One of ways to solve the problem of providing the industry with a sufficient amount of para-xylene is to obtain it via polymerization of *meta*- and *ortho*-xylenes and ethylbenzene and also via alkylation of benzene and toluene. The processes require that acid catalysts should be used. The most promising strategy for performing these catalytic transformations is based on using materials with a special elongated configuration of pores interconnected by narrow channels. A structure of this kind favors a more easy diffusion of para-xylene from pores into the ambient medium and, consequently, its higher yield in the course of synthesis. A structure of this kind is possessed by MFI (ZSM-5) or MOR zeolites and also by the increasingly popular zeolite of the MTW (ZSM-12) type, which was first obtained in 1974 by Mobil Oil [1]. This material

is characterized by a 1D system of channels formed by 12-member rings and  $5.7 \times 6.1 \text{ \AA}$  pores (Fig. 1).

A large number of studies concerned with synthesis and catalytic properties of ZSM-12 zeolite have been published [2–7]. The properties of the materials being synthesized, such as the particle morphology and activity in chosen catalytic processes, are largely determined by the choice of a template. Therefore, a search for new templates and analysis of how their structure affects the properties of the resulting zeolites seem to be topical tasks.

The present study is concerned with new types of templates, salts of ethanolamines (dimethyl ethanolamine and methyl diethanolamine), used to synthesize ZSM-12 zeolites. The materials obtained are examined by the methods of powder X-ray diffraction, scanning electron microscopy (SEM), IR spectroscopy, low-temperature adsorption–desorption of nitrogen, and elemental analysis. Also, the properties of the ZSM-12 zeolites synthesized with new templates with the materials obtained under similar conditions with the conventional templates, salts of tetraethylammonium and triethylmethylammonium.

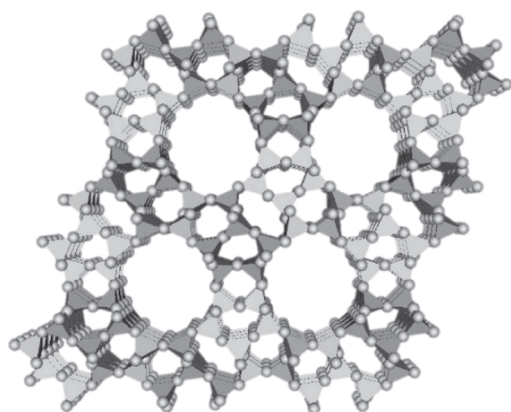


**Fig. 1.** Typical structure of the ZSM-12 zeolite.

## EXPERIMENTAL

The zeolites were synthesized from the following reagents: colloid solution of silicon oxide Ludox HS-40 (40 wt %, Sigma-Aldrich), aluminum sulfate octadecahydrate  $[\text{Al}_2(\text{SO}_4)_3 \cdot 18\text{H}_2\text{O}$ , Sigma-Aldrich, 99%), tetraethylammonium bromide ( $[\text{TEA}]\text{Br}$ , Sigma-Aldrich, 98%), methyltetraethylammonium chloride ( $[\text{MTEA}]\text{Cl}$ , Sigma-Aldrich, 97%), dimethylethanolamine  $[(\text{CH}_3)_2\text{NC}_2\text{H}_4\text{OH}$ , Sigma-Aldrich, 98%], methyltriethanolamine  $[\text{CH}_3\text{N}(\text{C}_2\text{H}_4\text{OH})_2$ , Sigma-Aldrich, 98%)], bromoethane ( $\text{C}_2\text{H}_5\text{Br}$ , Sigma-Aldrich, 99%), sodium hydroxide ( $\text{NaOH}$ , Komponent-Reaktiv, 98%, and ammonium chloride ( $\text{NH}_4\text{Cl}$ , Khimmed, 98%).

Synthesis of monoethanol-*N,N*-dimethyl-*N*-ethylammonium bromide  $[\text{DMER}(\text{EtOH})\text{A}]\text{Br}$ . A 50-mL flask equipped with the core of a magnetic rabble was charged with dimethylethanolamine (10.0 mL, 0.1 mol) and ethyl bromide (7.8 mL, 0.105 mol). The reaction was performed under agitation in the course of 12 h. The resulting mixture was evaporated under reduced pressure

in a rotary evaporator to remove the excess amount of ethyl bromide. A colorless amorphous product with a mass of 19.8 g was obtained.  $^1\text{H}$  NMR spectrum,  $\delta$  (ppm) ( $\text{DMSO}-d_6$ ): 1.22 (3H, t), 3.04 (6H, s), 3.37–3.41 (2H, q), 3.40–3.44 (2H, m), 3.79 (2H, br. s), 5.28 (1H, br.s).

**Synthesis of diethanol-*N*-methyl-*N*-ethylammonium bromide  $[\text{MED}(\text{EtOH})\text{A}]\text{Br}$ .** A 50-mL flask equipped with the core of a magnetic rabble was charged with methyldiethanolamine (11.5 mL, 0.1 mol) and ethyl bromide (7.8 mL, 0.105 mol). The reaction was performed under agitation in the course of 12 h. The resulting mixture was evaporated under reduced pressure in a rotary evaporator to remove the excess amount of ethyl bromide. A colorless amorphous product with a mass of 22.6 g was obtained.  $^1\text{H}$  NMR spectrum,  $\delta$  (ppm) ( $\text{DMSO}-d_6$ ): 1.22 (3H, t), 3.05 (3H, s), 3.37–3.41 (2H, q), 3.43–3.49 (4H, q), 3.77–3.81 (4H, m), 5.25 (2H, t).

ZSM-12 zeolites were synthesized by the previously described methods under hydrothermal conditions [5, 8]. The zeolites being synthesized are listed in Table 1. The typical procedure includes preparing a gel by mixing solutions containing aluminum sulfate, sodium hydroxide, and a template (solution 1,  $\text{H}_2\text{O} : \text{Al}_2\text{O}_3 : \text{template} : \text{Na}_2\text{O} = 1157.4 : 1 : 35 : 20.8$ ) and a colloid solution of silicon oxide (solution 2,  $\text{H}_2\text{O} : \text{SiO}_2 = 3.3 : 1$ ). Further, the gel was transferred into an autoclave equipped with a Teflon insert and the synthesis was performed under hydrothermal conditions in a drying box with air convection at a temperature of 155°C in the course of 120 h. The resulting product was washed with water to remove remains of the reaction mixture, dried, calcined, and an ion exchange was performed to obtain the  $\text{NH}_4$  form of the zeolite. A repeated drying and calcination of the product yielded a wide powder of the H form of ZSM-12 zeolites.

SEM micrographs of samples were obtained on a Hitachi TM3030 bench-top scanning electron microscope. The information about the local elemental composition and element distribution over the sample surface was obtained with an energy-dispersive spectrometer (EDX) with Quantax 70 hardware-software system.

The elemental analysis was made on a Thermo ARL PERFORM'X instrument with a 2500-V X-ray tube. Prior to an analysis, 200-mg samples were compacted into a pellet with boric acid.

The X-ray analysis was made on a Rigaku Rotaflex D/max-RC instrument with  $\text{CuK}\alpha$  radiation ( $\lambda = 0.154$  nm).

**Table 1.** Zeolites synthesized and examined in the study

Sample	$\text{SiO}_2/\text{Al}_2\text{O}_3$	Template
ZSM-12-A-280		$[\text{TEA}]\text{Br}$
ZSM-12-B-280		$[\text{MTEA}]\text{Cl}$
ZSM-12-C-280	280	$[\text{DME}(\text{EtOH})\text{A}]\text{Br}$
ZSM-12-D-280		$[\text{MED}(\text{EtOH})\text{A}]\text{Br}$
ZSM-12-B-140		$[\text{MTEA}]\text{Cl}$
ZSM-12-C-140	140	$[\text{DME}(\text{EtOH})\text{A}]\text{Br}$

The diffraction pattern of a sample was recorded at angles  $2\theta = 3\text{--}50^\circ$  with a step of  $0.04^\circ$  at a scanning rate of  $4 \text{ deg min}^{-1}$ . The degree of crystallinity was calculated from the ratio between the areas (integral intensities) of peaks associated with the crystalline and amorphous phases.

The nitrogen adsorption–desorption isotherms were recorded at a temperature of 77 K on a Micromeritics Gemini VII 2390 (V1.02t) instrument. Prior to measurements, samples were degassed at a temperature of  $300^\circ\text{C}$  for 6 h. The surface area was calculated by the Brunauer–Emmett–Teller (BET) method from adsorption data at relative pressures  $p/p_0 = 0.05\text{--}0.2$ . The total pore volume was determined from the amount of nitrogen adsorbed at a relative pressure  $p/p_0 = 0.95$ .

The acidity of the samples was determined with a Micromeritics AutoChem HP2950 instrument. For this purpose, a sample under study with 250–500- $\mu\text{m}$  granulometric composition and mass of about 300 mg was placed in a quartz reactor and blown-through with nitrogen at  $300^\circ\text{C}$  for 1 h. The saturation with ammonia was performed in a flow of an ammonia/nitrogen mixture of gases at a temperature of  $100^\circ\text{C}$  for 30 min. The physically adsorbed ammonia was removed at  $100^\circ\text{C}$  in a flow of nitrogen in the course of 30 min by blowing-through with helium at a rate of  $50 \text{ mL min}^{-1}$ . To obtain a temperature-programmed desorption curve,

the temperature was gradually raised to  $700^\circ\text{C}$  at a rate of  $10 \text{ deg min}^{-1}$ .

The zeolites were analyzed by Fourier transformed IR spectroscopy on a Thermo Scientific Nicolet IR2000 instrument with multiple frustrated total internal reflection with a Multireflection HATR attachment containing a  $45^\circ$  ZnSe crystal for various wavelength ranges with a resolution of 4 nm.

## RESULTS AND DISCUSSION

The diffraction patterns of the zeolite samples obtained at different Si/Al ratios with various templates are presented in Fig. 2. Signals characteristic of the ZSM-12 zeolite are observed in all cases, which confirms that the required product is formed. All the peaks indicate that a material is formed with a crystal lattice of monoclinic  $C2/c$  crystallographic system, which corresponds to the structure first obtained by researchers from Mobil [1, 9, 10]. In addition, the absence of a rise in peaks at  $2\theta = 17\text{--}30^\circ$  is indicative of the large degree of crystallinity of the resulting zeolites. It should also be noted that nearly all the zeolite samples contain a minor amount of the ZSM-5 impurity phase.

IR spectroscopic data also confirm that the zeolites synthesized in the study belong to the MTW class with ZSM-12 structure (Fig. 3). The spectra of all the zeolites

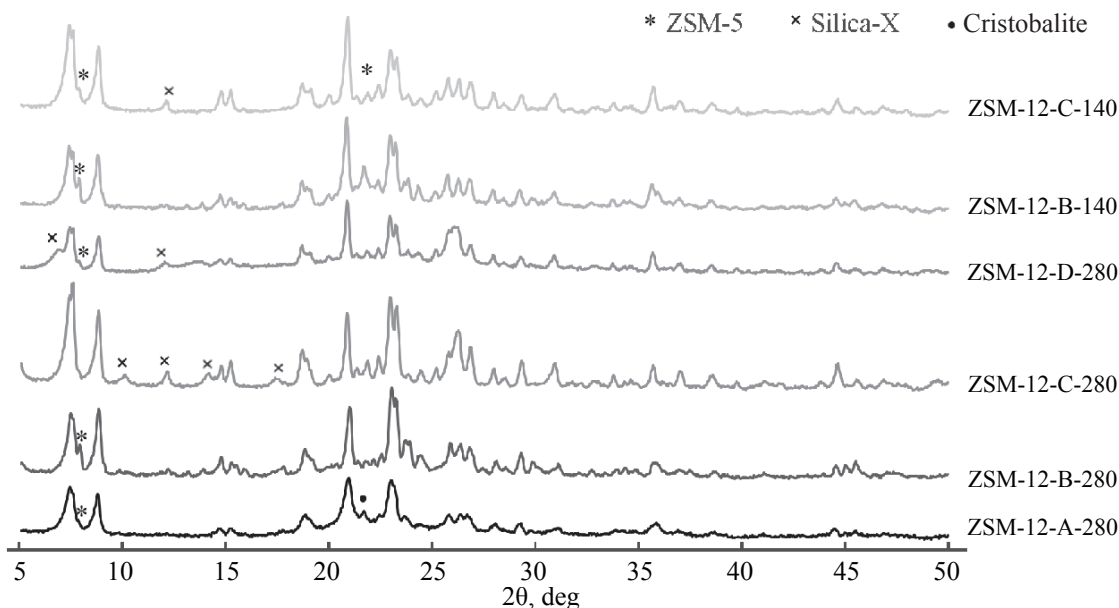


**Fig. 2.** Diffraction patterns of samples of the zeolites synthesized in the study.

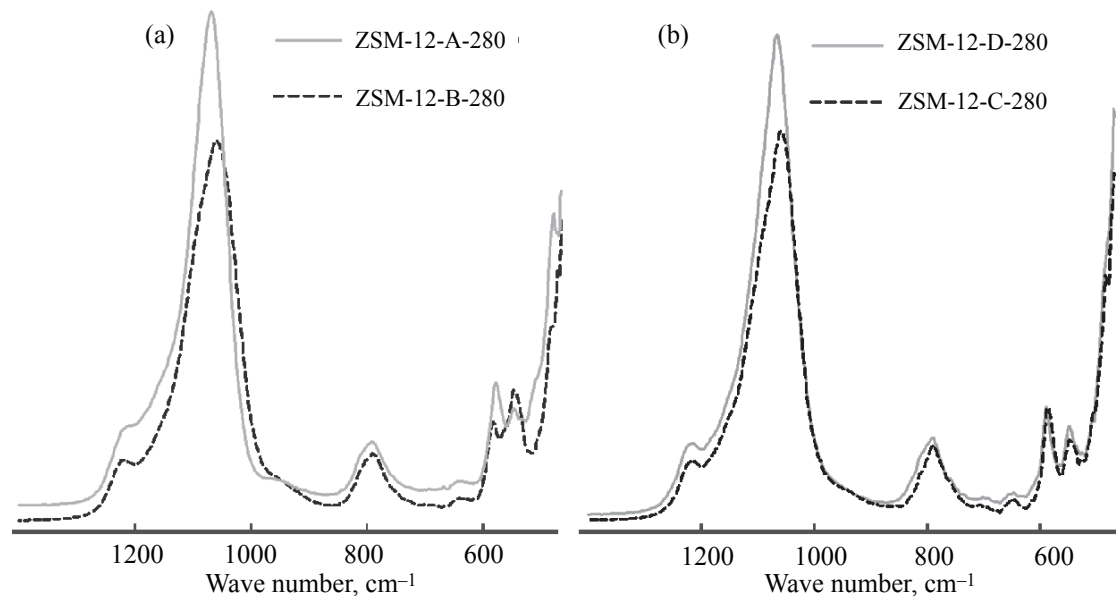


**Fig. 3.** IR spectra of ZSM-12 zeolites: (a) ZSM-12-A-280 and ZSM-12-B-280 and (b) ZSM-12-C-280 and ZSM-12-D-280.

contain at 450–1400 cm<sup>-1</sup> a number of absorption bands characteristic of ZSM-12 materials, peaked at 480 ( $\delta_b$  O—Si—O), 543, 580 ( $\nu_s$  Si—O—Si +  $\delta$  O—Si—O), 640 ( $\nu_s$  Si—O—Al), 785 ( $\nu_s$  Si—O—Si), 1060–1068 [ $\nu_{as}$  Si—O(Si/Al), in the bulk of the material], and 1211–1220 cm<sup>-1</sup> [ $\nu_{as}$  Si—O(Si/Al), on the surface of the material]. The presence of absorption bands at 543, 580, and 640 cm<sup>-1</sup> directly evidence that the material has structures formed by a prism with bases formed by 12-member rings. These data agree with those obtained previously [11, 12].

The porosity characteristics of the materials were examined by the method of low-temperature adsorption–

desorption of nitrogen. A typical run of the nitrogen adsorption–desorption curves for the materials obtained is shown in Fig. 4. At low pressures ( $p/p_0 = 0$ –0.05), there is a strong absorption of nitrogen, which indicates that there are micropores in the structure of the zeolites. In some cases, the curves show a small hysteresis between the adsorption and desorption curves, which is characteristic of mesoporous materials. The presence of mesopores with average size of about 3.6–3.8 nm may be due to the formation of voids in aggregation of several crystallites in the course of the hydrothermal synthesis [12–15]. The zeolites have large values of the specific surface area and pore volume, presented below.

Figure 5 shows SEM micrographs of the zeolites and the average crystal size of each of these. It is noteworthy that different crystallite shapes are observed for zeolites synthesized with various templates, which is due to the different mechanisms of interaction of template molecules with silicon dioxide in the course of the crystallization [16]. A spherical/cubic particle shape and a rather narrow particle size distribution are characteristic of ZSM-12-A-280 (Fig. 5a). Materials with a similar morphology have also been obtained with templates based on tetraethylammonium {2, 3, 17, 18]. The crystals of ZSM-12-B-280 and ZSM-12-B-140 zeolites (Figs. 5b and 5c) are rather widely distributed over sizes and shapes: both rather small particles that resemble in shape rice grains and well formed coarse crystals are observed. The particle shape similar to a rice grain of zeolites produces

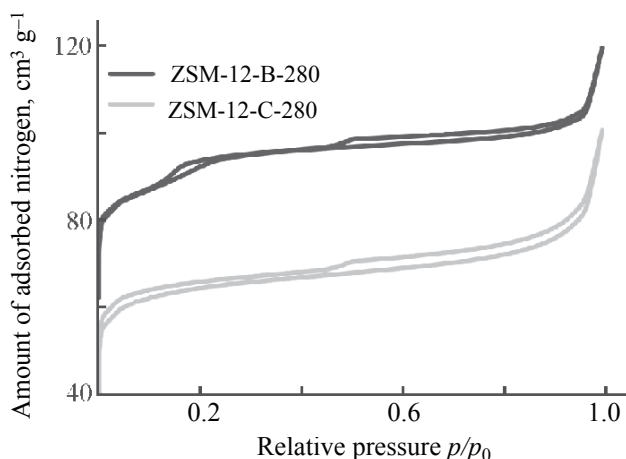


**Fig. 4.** Typical run of the nitrogen adsorption–desorption curves for ZSM-12 zeolites for the example of ZSM-12-B-280 and ZSM-12-C-280 materials.

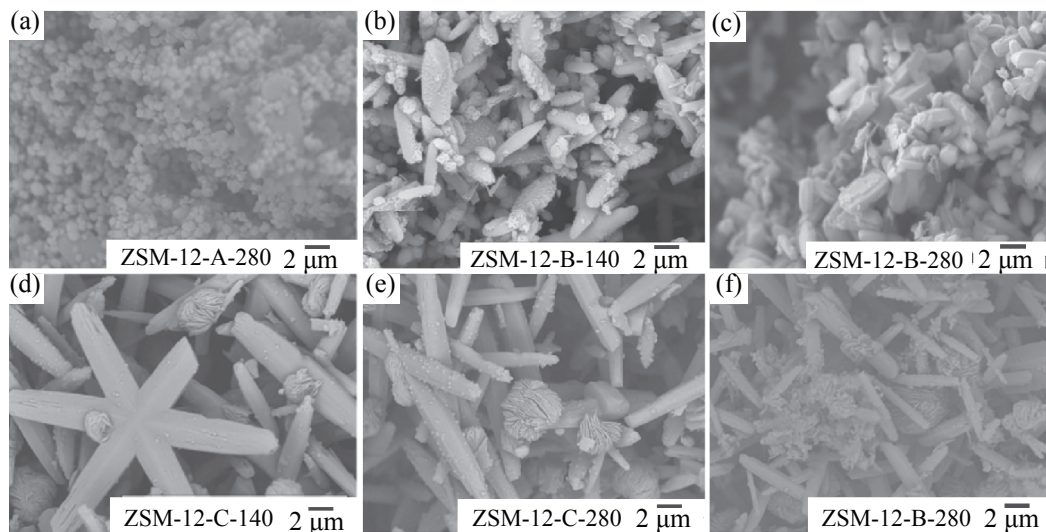


**Fig. 5.** SEM micrographs of the zeolites (a) ZSM-12-A-280, (b) ZSM-12-B-140, (c) ZSM-12-B-280, (d) ZSM-12-C-140, (e) ZSM-12-C-280, (f) ZSM-12-D-280.

with this template also agrees with previously published data [14, 18]. For the ZSM-12-C-140, ZSM-12-D-280, and ZSM-12-D-280 zeolites, the crystallites have an elongated shape with a rather narrow size distribution. An acicular, well formed shape of crystals with a hexagonal morphology is observed.

The main characteristics of the zeolites are listed in Table 2. It is noteworthy that, according to the results of an elemental analysis, the Si/Al ratio in the materials synthesized is smaller than the calculated value. This phenomenon, possibly due to the incomplete transformation of silicon dioxide from the colloid form to the crystalline phase in the course of the crystallization process, was also observed in a number of other studies [19–21].

## CONCLUSIONS

ZSM-12 zeolites were synthesized with ethanolamine salts used as templates. It was shown that the structure of templates strongly affects the properties of the materials obtained: materials based on the “conventional” templates, salts of tetraethylammonium and triethylmethylammonium have a cubic and spherical morphology of their crystallites and are characterized by, on the whole, smaller particle size and larger surface area and pore volume. At the same time, zeolites obtained on the basis of the new templates have a substantially better formed shape of crystals, which may be due to the stronger interaction of template molecules with the zeolite material in the course of crystallization.

**Table 2.** Characteristics of the zeolites

Zeolite	Surface area by BET, m <sup>2</sup> g <sup>-1</sup>	Pore volume, cm <sup>3</sup> g <sup>-1</sup>	Elemental composition	Average crystallite size, μm
ZSM-12-A-280	187	0.12	0.08Na <sub>2</sub> O : Al <sub>2</sub> O <sub>3</sub> : 185SiO <sub>2</sub>	0.9
ZSM-12-B-140	262	0.11	0.1Na <sub>2</sub> O : Al <sub>2</sub> O <sub>3</sub> : 117SiO <sub>2</sub>	4.4
ZSM-12-B-280	274	0.13	0.2Na <sub>2</sub> O : Al <sub>2</sub> O <sub>3</sub> : 226SiO <sub>2</sub>	3.6
ZSM-12-C-140	196	0.06	0.02Na <sub>2</sub> O : Al <sub>2</sub> O <sub>3</sub> : 126SiO <sub>2</sub>	8.5
ZSM-12-C-280	188	0.09	0.11Na <sub>2</sub> O : Al <sub>2</sub> O <sub>3</sub> : 201SiO <sub>2</sub>	11.2
ZSM-12-D-280	183	0.07	0.16Na <sub>2</sub> O : Al <sub>2</sub> O <sub>3</sub> : 217SiO <sub>2</sub>	6.1

## ACKNOWLEDGMENTS

The study was financially supported by the Ministry of Education and Science of the Russian Federation, Federal target program “Research and development in priority areas of the scientific-technological complex of Russia for the years of 2014–2020,” Arrangement 1.4, Subsidy agreement no. 14.610.21.0009 of 0.3.10.2017. Unique agreement identifier RFMEFI61017X0009.

## REFERENCES

1. US Patent 3 832 449 (publ. 1974).
2. Dimitrov, L., Mihaylov, M., Hadjiivanov, K., Mavrodinova, V., *Microporous Mesoporous Mater.*, Elsevier Inc., 2011, vol. 143, nos. 2–3, pp. 291–301.
3. Jegatheeswaran, S., Cheng, C.M., and Cheng, C.H., *Microporous Mesoporous Mater.*, Elsevier Inc., 2015, vol. 201, no. C, pp. 24–34.
4. Li, J., Lou, L.-L., Xu, C., and Liu, S., *Catal. Commun., Elsevier B, V*, 2014, vol. 50, pp. 97–100.
5. Sanhoob, M.A., Muraza, O., Taniguchi, T., Tago, T., Watanabe, G., and Masuda, T., *Microporous Mesoporous Mater.*, 2014, vol. 194, pp. 31–37.
6. Massoumifard, N., Kaliaguine, S., and Kleitz, F., *Microporous Mesoporous Mater.*, 2016, vol. 227, pp. 258–271.
7. Chaves, T.F., Carvalho, K.T.G., Urquiza-González, E.A., and Cardozo, D., *Catal. Lett.*, 2016, vol. 146, no. 10, pp. 2200–2213.
8. Sanhoob, M.A., Muraza, O., Al-Mutairi, E.M., and Ullah, N., *Adv. Powder Technol. Soc., Powder Technol. Japan*, 2015, vol. 26, no. 1, pp. 188–192.
9. Kinski, I., Daniels, P., Deroche, C., Marler, B., and Gies, H., *Microporous Mesoporous Mater.*, 2002, vol. 56, no. 1, pp. 11–25.
10. US Patent 4 452 769 (publ. 1983).
11. Zhu, H.-B., Xia, Q.-H., Guo, X.-T., Su, K.-X., Hu, D., Ma, X., Zeng, D., and Deng, F., *Mater. Lett.*, 2006, vol. 60, nos. 17–18, pp. 2161–2166.
12. Wu, W., Wu, W., Kikhtyanin, O.V., Li, L., Toktarev, A.V., Ayupov, A.B., Khabibulin, J.F., Echevsky, G.V., and Huang, J., *Appl. Catal. A*, 2010, vol. 375, no. 2, pp. 279–288.
13. Carvalho, K.T.G. and Urquiza-González, E.A., *Catal. Today*, 2015, vol. 243, no. 1, pp. 92–102.
14. Chiche, B.H., Dutartre, R., Di Renzo, F., and Fajula, F., *Catal. Lett.*, 1995, vol. 31, no. 4, pp. 359–366.
15. Xia, Q.-H., Shen, S.-C., Song, J., Kawi, S., and Hidajat, K., *J. Catal.*, 2003, vol. 219, no. 1, pp. 74–84.
16. Ritsch, S., Ohnishi, N., Ohsuna, T., Hiraga, K., Terasaki, O., Kubota, Y., and Sugi, Y., *Chem. Mater.*, 1998, vol. 10, no. 12, pp. 3958–3965.
17. Zhao, Y., Zhang, H., Wang, P., Xue, F., Ye, Z., Zhang, Y., and Tang, Y., *Chem. Mater.*, 2017, vol. 29, no. 8, pp. 3387–3396.
18. Mehla, S., Krishnamurthy, K.R., Viswanathan, B., John, M., Niwate, Y., Kishore Kumar, S.A., Pai, S.M., and Newalkar, B.L., *Microporous Mesoporous Mater.*, Elsevier Inc., 2013, vol. 177, pp. 120–126.
19. Souza, M.J.B., Silva, A.O.S., Garrido Pedrosa, A.M., and Araujo, A.S., *React. Kinet. Catal. Lett.*, 2005, vol. 84, no. 2, pp. 287–293.
20. Araujo, A.S., Silva, A.O.S., Souza, M.J.B., Coutinho, A.C.S.L.S., Aquino, J.M.F.B., Moura, J.A., and Pedrosa, A.M.G., *Adsorption*, 2005, vol. 11, no. 2. Spec. Issue, pp. 159–165.
21. Gopal, S., Yoo, K., and Smirniotis, P.G., *Microporous Mesoporous Mater.*, 2001, vol. 49, nos. 1–3, pp. 149–156.